Science
AAAS

White Fat Progenitor Cells Reside in the Adipose Vasculature
Wei Tang, *et al.*
Science **322**, 583 (2008);
DOI: 10.1126/science.1156232

Science (print ISSN 0036-8075; online ISSN 1095-9203) is published weekly, except the last week in December, by the American Association for the Advancement of Science, 1200 New York Avenue NW, Washington, DC 20005.

White Fat Progenitor Cells Reside in the Adipose Vasculature

Wei Tang,[1] Daniel Zeve,[1] Jae Myoung Suh,[1] Darko Bosnakovski,[1] Michael Kyba,[1] Robert E. Hammer,[2] Michelle D. Tallquist,[3] Jonathan M. Graff[1,3,4]*

White adipose (fat) tissues regulate metabolism, reproduction, and life span. Adipocytes form throughout life, with the most marked expansion of the lineage occurring during the postnatal period. Adipocytes develop in coordination with the vasculature, but the identity and location of white adipocyte progenitor cells in vivo are unknown. We used genetically marked mice to isolate proliferating and renewing adipogenic progenitors. We found that most adipocytes descend from a pool of these proliferating progenitors that are already committed, either prenatally or early in postnatal life. These progenitors reside in the mural cell compartment of the adipose vasculature, but not in the vasculature of other tissues. Thus, the adipose vasculature appears to function as a progenitor niche and may provide signals for adipocyte development.

How adipocytes (fat cells) develop is a fundamental biological question with important ramifications for human health and disease (*1*, *2*). Little is known about the identity, localization, or biological characteristics of endogenous adipocyte progenitors (*2*). These progenitors probably reside in the adipose stromal-vascular fraction (SVF), a heterogeneous mixture of cells operationally defined by enzymatic dissociation of adipose depots followed by density separation from adipocytes (*1*, *3*). Peroxisome proliferator-activated receptor gamma (PPARγ), a central regulator of fat formation, is necessary and sufficient for adipogenesis (*4*, *5*). Thus, marking PPARγ-expressing cells in vivo might provide insights into adipose lineage specification.

To mark and perform lineage analyses on PPARγ-expressing cells, we generated PPARγ–tet transactivator (tTA) (*6*) knock-in mice placing tTA under the control of the PPARγ locus (fig. S1) (*7*). We introduced into these PPARγ-tTA mice two additional alleles: (i) a tTA-responsive Cre allele [tetracycline response element-Cre (TRE-Cre)] and (ii) an element that indelibly expresses lacZ in response to the Cre recombinase (ROSA26-flox-stop-flox-lacZ) (*8*, *9*). With these genetic manipulations, we thereby created a PPARγ-reporter strain (PPARγ-R26R, for PPARγ-Rosa26 reporter) in which the endogenous PPARγ promoter/enhancer induces expression of tTA, leading to Cre expression and an indelible lacZ marking of PPARγ-expressing cells and all descendants (fig. S1). The PPARγ-tTA strain functioned as expected; that is, it was active in adipose depots and repressed by doxycycline (Dox), establishing a tool to examine the adipose lineage (Fig. 1A and figs. S1 and S2).

To capture the rapid and dramatic expansion of the adipose lineage that occurs during the first postnatal month (*1*, *10*), we Dox-treated the PPARγ-R26R mice, starting at different days during this crucial window (fig. S3A). We found

[1]Department of Developmental Biology, University of Texas Southwestern Medical Center, Dallas, TX 75390, USA. [2]Department of Biochemistry, University of Texas Southwestern Medical Center, Dallas, TX 75390, USA. [3]Department of Molecular Biology, University of Texas Southwestern Medical Center, Dallas, TX 75390, USA. [4]Department of Internal Medicine, University of Texas Southwestern Medical Center, Dallas, TX 75390, USA.

*To whom correspondence should be addressed. E-mail: jon.graff@utsouthwestern.edu

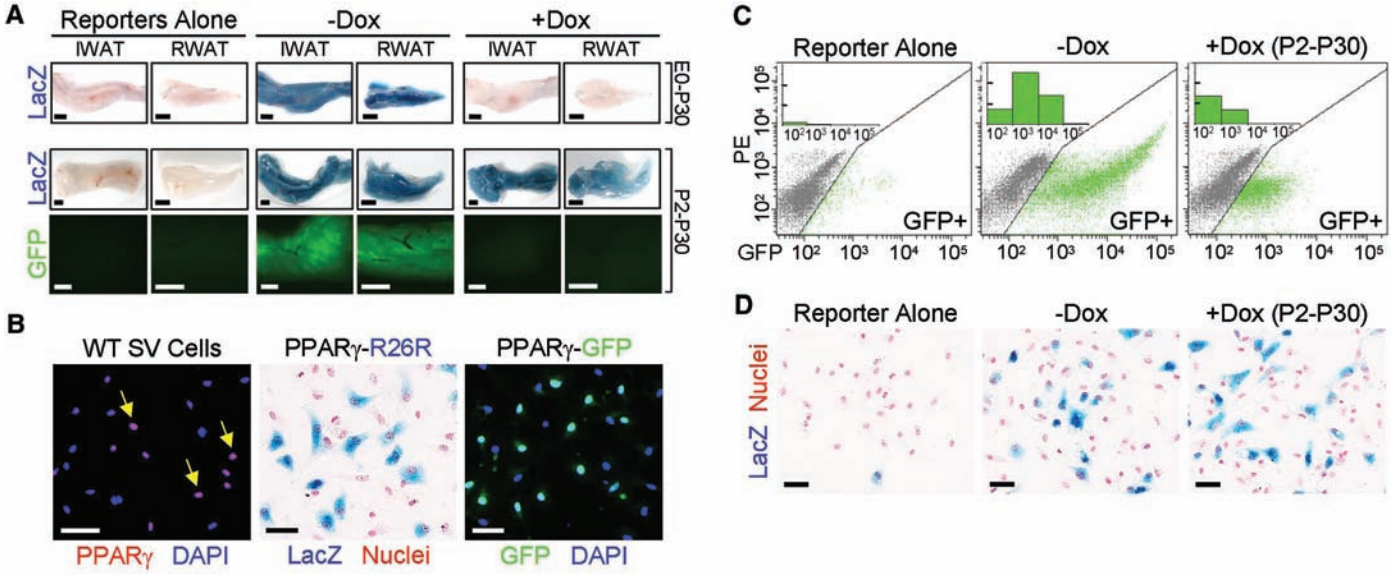

Fig. 1. PPARγ-expressing progenitors proliferate and maintain the precursor pool. (**A**) PPARγ-tTA;TRE-Cre;R26R (PPARγ-R26R) or PPARγ-tTA;TRE-H2B-GFP (PPARγ-GFP) (bottom panels) mice were treated with or without Dox, either from embryonic day 0 (E0) to postnatal day 30 (P30) (top row) or from P2 to P30 (middle and bottom rows), and then inguinal and retroperitoneal white adipose tissues (IWAT and RWAT, respectively) were excised and examined for lacZ (blue) or GFP (green) expression. Left panels show equivalent depots of control mice containing either TRE-Cre;R26R or TRE-H2B-GFP. (**B**) P30 SV cells from wild-type (left), PPARγ-R26R (middle), and PPARγ-GFP (right) WAT were examined for expression of PPARγ (red) with immunocytochemistry (left) or for reporter expression. (Left) Nuclei were stained with 4′,6′-diamidino-2-phenylindole (DAPI) (blue). Yellow arrows indicate cells that express PPARγ (purple). (Middle) lacZ (blue) nuclei counterstained with nuclear fast red (red). (Right) GFP (green) nuclei stained with DAPI (blue). (**C**) Flow cytometry profiles of SV cells of untreated TRE-H2B-GFP (left) or PPARγ-GFP mice treated without (middle) or with Dox (right) from P2 to P30. The *x* axis is GFP fluorescent intensity, and the *y* axis is phycoerythrin (PE) channel to help illustrate the distribution of GFP$^+$ cells. (Inset) The *x* axis is GFP fluorescent intensity, and the *y* axis is the cell count of the GFP$^+$ cells per interval of fluorescent intensity (one unit = 1000). SV cells from TRE-H2B-GFP mice served as a gating control. (**D**) SV cells removed from TRE-Cre;R26R (left) and PPARγ-R26R mice treated as indicated were isolated and stained with X-Gal (blue) and nuclear fast red (red). Dox treatment did not alter the number or percentage of lacZ$^+$ cells based on statistical analysis of more than 2000 cells counted in each group. Scale bars: (A), 2 mm; (B) and (D), 50 μm.

homogenous lacZ expression in postnatal day 30 (P30) adipose depots that was not appreciably altered, even when Dox administration began in the first postnatal days (Fig. 1A and fig. S3). This surprising result indicated that the vast majority of P30 adipocytes derived from a preexisting pool of PPARγ-expressing cells, either adipocytes already present prenatally/early postnatally or proliferating precursors. Both interpretations conflict with previous data, however. The possibility that these cells are pre-formed adipocytes is incompatible with the proliferative increase that occurs over this time frame, whereas the notion that PPARγ-expressing cells are progenitors is inconsistent with cell culture studies (*11*, *12*). To distinguish between the two possible interpretations, we examined the Dox-induced response of another reporter, TRE-H2B-GFP, that is stable in postmitotic cells but, in contrast to the indelible lacZ marker, becomes diluted in proliferating cells after inhibition of the tet system (*13*, *14*). Dox treatment (P2 to P30) markedly reduced adipose depot and adipocyte green fluorescent protein (GFP) expression (Fig. 1A), indicating that PPARγ-expressing cells proliferate. Consistent with these data, ~50% of adipocytes were labeled by bromodeoxyuridine (BrdU) when administered between P10 and P30 (fig. S4). The stability of lacZ marking together with the diminishing GFP expression indicate that adipose lineage cells, already instructed to express PPARγ prenatally, proliferate and are the major source of the spurt of adipocyte development observed in the first month of life.

The adipose SVF (fig. S5) is postulated to contain adipocyte progenitors (*1*, *15*). We therefore investigated this location as a possible source from which the proliferating PPARγ-expressing cells characterized above may originate. We found that a subset of stromal-vascular (SV) cells expressed immunocytochemically detectable levels of PPARγ, as well as the lacZ and GFP reporters (Fig. 1B and fig. S6). These SV resident PPARγ-expressing cells proliferate, as they incorporated BrdU after a brief 2-hour chase, even when the BrdU pulse-chase was initiated after 10 days of Dox pretreatment to ensure that cells containing both GFP and BrdU expressed GFP before initiation of the brief BrdU pulse (fig. S7). In addition, GFP^+ SV cells isolated by fluorescence-activated cell sorting (FACS) had considerable proliferative capacity (fig. S8). Further support for the in vivo proliferation of the GFP^+ SV cells derives from flow cytometry profiles showing a Dox-induced (P2 to P30) decrease in the number and fluorescent intensity of GFP^+ SV cells (Fig. 1C and fig. S9). Dox did not reduce the number or percentage of $lacZ^+$ SV cells, indicating that a pool of PPARγ-expressing cells remains in the SV compartment (Fig. 1D). Together these data indicate that the SV compartment of adipose depots contains PPARγ-expressing cells that divide, are mobilized from and also repopulate the SVF, and behave as an amplifying population that contributes to the adipocyte lineage.

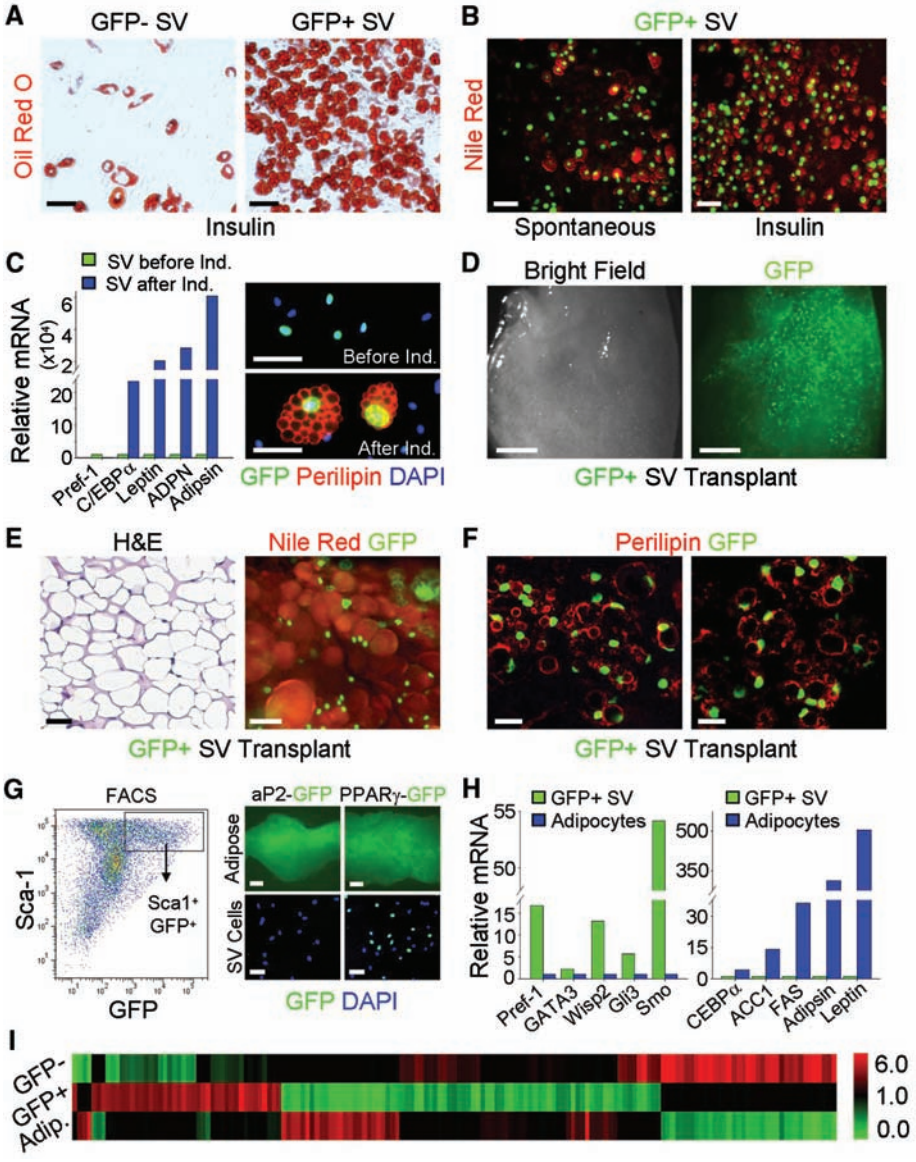

Fig. 2. PPARγ-expressing SV cells are adipogenic and have a unique molecular signature. (**A**) GFP^- and GFP^+ SV cells from PPARγ-GFP mice were sorted, plated, cultured to confluence, and insulin-stimulated adipogenesis was examined with the lipid-specific stain Oil Red O (red). (**B**) Sorted GFP^+ SV cells were cultured in media or media supplemented with insulin and then stained with Nile red, a lipid-specific fluorescent dye, to simultaneously visualize fat accumulation and GFP expression. (**C**) (Left) Quantitative real-time fluorescence polymerase chain reaction (QPCR) analysis of the indicated markers in sorted GFP^+ cells before (green bars) and after (blue bars) insulin-stimulated adipogenesis. C/EBPα is an adipogenic transcription factor; leptin, adiponectin (ADPN), and adipsin are adipokines; and Pref-1 is a preadipocyte marker whose expression inversely correlates with adipogenesis. (Right) SV cells from P30 PPARγ-GFP adipose depots were examined for GFP (green) and perilipin (an adipocyte marker, red) expression both before (top) and after (bottom) adipogenic induction. Nuclei were stained with DAPI (blue). (**D** to **F**) FACS-isolated GFP^+ SV cells were implanted into nude mice, and the tissue that formed after 1 month was photographed with bright field [left panel in (D)] and fluorescent microscopy [right panel in (D)] and examined with hematoxylin and eosin (H&E) staining [left panel in (E)], GFP fluorescence and Nile red staining [right panel in (E)], and GFP fluorescence and perilipin immunochemistry (F). (**G**) (Left) P30 PPARγ-GFP adipose depot SV cells were examined for Sca-1 and GFP expression with flow cytometry. The box indicates the $Sca1^+GFP^+$ double-positive population. (Right) IWAT (adipose, top) and SV cells (bottom) of aP2-GFP transgenics were analyzed for GFP expression, which was present in adipocytes but not in SV cells. PPARγ-GFP serves as a control. Nuclei were stained with DAPI (blue). (**H**) QPCR analyses of the indicated markers of FACS-isolated GFP^+ SV cells (green bars) and floated adipocytes (blue bars). (**I**) GFP^- SV cells, GFP^+ SV cells, and adipocytes were subjected to gene-expression profiling. The heat map illustrates 152 genes that differentiate GFP^+ SV cells from the other populations. Red depicts a greater-than-or-equal-to twofold increase in gene expression, whereas green depicts a less-than-or-equal-to twofold decrease in gene expression. Scale bars: (A) to (C), (E), and right panel, bottom row of (G), 50 μm; (D) and right panel, top row of (G), 2 mm; (F), 20 μm in confocal images.

We assessed the adipogenic potential (in vitro and after transplantation) of FACS-isolated GFP$^+$ SV cells (fig. S10). In culture, the sorted GFP$^+$ SV cells underwent spontaneous and insulin-stimulated adipogenesis that was enhanced compared with GFP$^-$ SV cells (Fig. 2, A and B, and fig. S11). GFP$^+$ SV adipogenesis mirrored the gene-expression patterns described for preadipocyte cell line adipogenesis, and the induced adipocytes expressed the perilipin protein with the appropriate subcellular distribution (Fig. 2C) (*16*). Moreover, freshly isolated GFP$^+$ P30 SV cells transplanted into nude mice led to formation of an ectopic GFP$^+$ depot, containing lipid-laden adipocytes that coexpressed GFP and perilipin (Fig. 2, D to F). Thus these GFP$^+$ SV cells have the proliferative and adipogenic properties expected of the endogenous progenitor population.

To characterize the GFP$^+$ SV progenitors and their relationship to other cells present in the adipose depot, we assessed cell-surface marker expression using flow cytometry and FACS (fig. S10). The majority of GFP$^+$ SV cells expressed Sca1 and CD34, but not CD105, CD45, TER-119, or Mac-1 (Fig. 2G and fig. S12). When these markers were used to positively or negatively select cells (and independently of the GFP reporter), we again isolated a subset of SV cells that generated a GFP$^+$ ectopic adipose depot after transplantation (fig. S13). Some GFP$^+$ SV cells could potentially be differentiated adipocytes that had yet to accumulate enough lipid to float during the density-based SV fractionation procedure. However, reporters driven by the promoter/enhancer of aP2 (*17*), a marker of adipocytes and a PPARγ target gene, displayed strong expression in adipose depots and adipocytes but not in SV cells, unlike the PPARγ reporters (Fig. 2G and fig. S14). Immunocytochemical analyses also showed that the GFP$^+$ SV cells did not express perilipin, an adipocyte marker (Fig. 2C). In addition, the FACS-isolated GFP$^+$ SV cells were molecularly distinct from adipocytes, expressing higher levels of the preadipocyte marker Pref-1, the adipogenic inhibitor GATA3, and targets of the anti-adipogenic Wnt (Wisp2) and Hedgehog (Smo, Gli3) pathways and much lower levels of numerous adipocyte markers (e.g., C/EBPα, FAS, leptin, etc.) (Fig. 2H and fig. S15A). Gene-expression profiles further defined the GFP$^+$ SV cells as a unique population within adipose tissues (Fig. 2I). Differentially expressed genes include developmental transcription factors (e.g., goosecoid and Twist2), extracellular matrix genes (e.g., MMP3), anti-angiogenic factors (e.g., Stab1), and signaling cascade components (e.g., EGFR and FGF10) (fig. S15B). Thus, GFP$^+$ SV

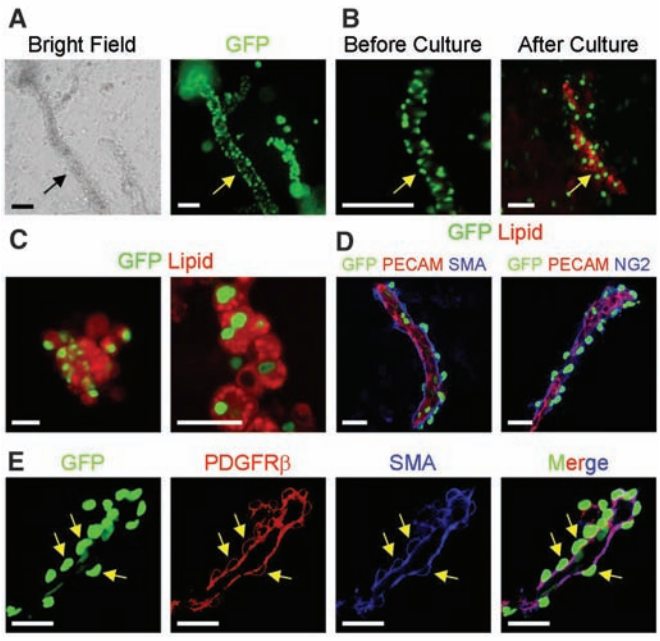

Fig. 3. SVP vessels contain GFP$^+$ precursors that form adipocytes. (**A**) SVP structures from P30 PPARγ-GFP mice were photographed with light (left) and fluorescent (right) microscopy. Arrows indicate an SV tube. (**B**) PPARγ-GFP SVP tubes were isolated and stained with the lipid-specific dye boron-dipyrromethene (BODIPY), either before culture (left) or after 3 days cultured on a petri dish in insulin (right). Arrows indicate an SV tube. (**C**) PPARγ-GFP SVP tubes were cultured in suspension. Formation of adipocytes that derive from the GFP$^+$ tubes was assessed with BODIPY staining (red). GFP is shown in green. Lipid droplets were visualized with confocal microscopy (right). (**D**) SVP isolates of P30 PPARγ-GFP mice were examined for expression of GFP (green) and the indicated endothelial (PECAM, red) and mural cell (SMA and NG2, blue) markers. (**E**) PPARγ-GFP SVP vessel was examined for expression of GFP (green) and the mural cell markers PDGFRβ (red) and SMA (blue). Yellow arrows indicate the position of GFP$^+$ nuclei within mural cells. Scale bars: (A), (B), and left panels of (C), 50 μm; right panels of (C), (D) and (E), 20 μm in confocal images.

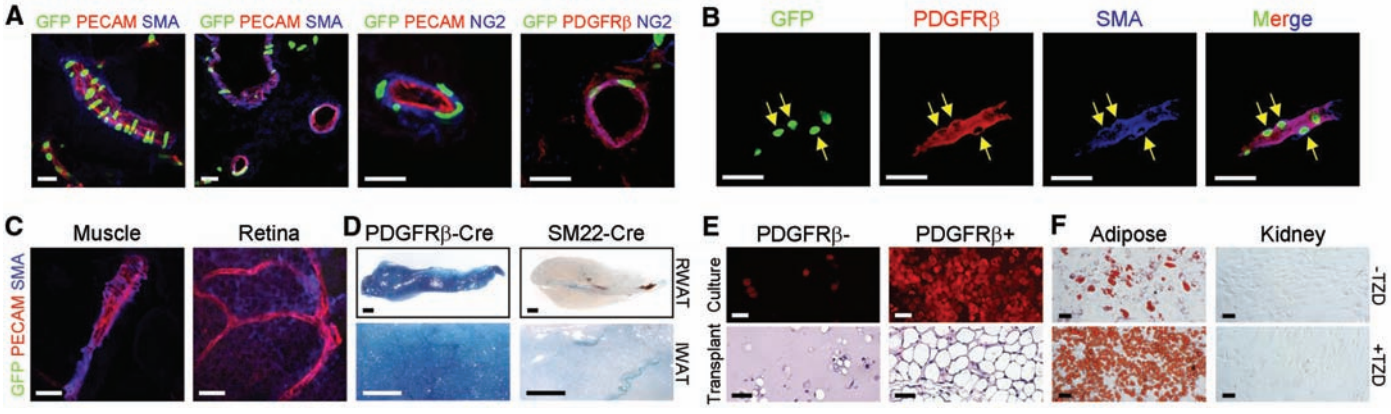

Fig. 4. GFP$^+$ cells are present in adipose depot mural cells. (**A**) P30 PPARγ-GFP WAT was freshly frozen, cryosectioned, and examined with direct fluorescence for GFP and indirect immunofluorescence for the indicated endothelial (PECAM, red) and mural cell (SMA, blue; NG2, blue; PDGFRβ, red) markers. (**B**) Cryosection of a PPARγ-GFP adipose depot showing expression of GFP, PDGFRβ (red), and SMA (blue). Yellow arrows indicate some mural cell nuclei that express GFP. (**C**) Muscle cryosections and retinal whole mount of PPARγ-GFP mice were examined for GFP, PECAM, and SMA as in (A) and (B). GFP was not expressed in mural cells of these tissues. (**D**) RWAT (top, ×5) and IWAT (bottom, ×20) of P30 PDGFRβ-Cre;R26R and SM22-Cre;R26R mice were stained for β-galactosidase expression (blue). (**E**) SV cells were isolated from P30 wild-type mice and sorted with a PDGFRβ antibody. (Top) Confluent PDGFRβ-negative and -positive cells were cultured in insulin, and fat formation was assessed with BODIPY (red). (Bottom) PDGFRβ-negative and -positive cells were transplanted into nude mice, and the resultant tissues were sectioned and H&E stained. (**F**) Adipose SVF and cells dissociated from the kidney were sorted with a PDGFRβ antibody, and PDGFRβ-positive cells were cultured in the absence (top) or presence (bottom) of TZD. Scale bars: (A) to (C), 20 μm in confocal images; (D), 1 mm; (E) and (F), 50 μm.

cells are phenotypically distinct from adipocytes and other SV cells and have a unique molecular signature that allows prospective isolation for transplantation and further lineage analyses.

The local microenvironment (niche) is a crucial determinant of progenitor fate, function, and maintenance (*18*). In part due to the nature of the SV dissociation and isolation method, the anatomical location and neighboring cells of the SV adipocyte precursors are not known. To investigate the architecture of the SV compartment, we developed an SV particulate (SVP) isolation procedure designed to partially maintain the native SV structure while removing adipocytes that obscure visualization of the precursor location (fig. S16). In the SVPs, the majority of GFP^+ cells were arrayed in tubelike structures (Fig. 3A). Based on inspection and lack of lipid staining, the GFP^+ cells present in freshly isolated tubes did not contain lipid droplets (Fig. 3, A and B). Organotypic cultures of SVPs led to formation of lipid-laden GFP^+ adipocytes along the tubes, indicating that the tube-associated SVP GFP^+ cells were adipogenic (Fig. 3, B and C). Because the SVP tubes resembled blood vessels, we stained them with antibodies that recognize constituent cells of the vasculature, including platelet endothelial cell adhesion molecule (PECAM) and three mural cell markers (SMA, PDGFRβ, and NG2) (*19*). The SVP tubes expressed PECAM and were surrounded by cells that expressed SMA, PDGFRβ, and NG2, indicating that they were vessels (Fig. 3, D and E). GFP^+ SVP cells expressed these mural cell markers (Fig. 3, D and E). The notion that PPARγ might be expressed in a subset of mural cells is noteworthy because cultured mural cells, similar to mesenchymal stem cells, are multipotent and can be induced to undergo adipogenesis, chondrogenesis, osteogenesis, and myogenesis and may provide a progenitor reservoir (*19*, *20*).

To investigate the distribution of the GFP^+ progenitors within the mural cell compartment, we immunohistochemically examined sections of freshly frozen PPARγ-GFP P30 adipose depots and other organs. In the adipose vasculature, we again observed colocalization of GFP and mural cell markers (Fig. 4, A and B). The GFP^+ vessels were of various sizes and disseminated throughout the depot (Fig. 4A). However, only a subset of mural cells within a vessel expressed GFP, and some adipose vessels did not appear to harbor GFP^+ progenitors (fig. S17). Mural cells in other examined P30 tissues (including skeletal and cardiac muscles, kidney, retina, pancreas, spleen, lung, etc.) did not express the GFP reporter (Fig. 4C and fig. S18). In older animals (~6 months), we detected GFP in some small caliber PECAM-positive, SMA-negative adult skeletal muscle vessels (figs. S19 and S20). The majority of these adult skeletal muscle GFP^+ cells expressed PECAM, and the cells were not adipogenic (fig. S20). Thus, adipose depots appear to contain a unique population of progenitors present in the adipose depot mural cell compartment.

PDGFRβ marks mural cells and is required for their development (*19*). To explore the possibility that PDGFRβ-expressing cells were part of the adipocyte lineage, we used β-galactosidase (X-Gal) to stain adipose depots of P30 mice that contained both a PDGFRβ-Cre transgene (*21*), which expresses Cre in mural cells and other developing cells, and R26R. As a specificity control, we used SM22-Cre (*22*), a driver construct expressed in a subset of vascular smooth muscle cells. In these Cre-mediated lineage studies, we found that PDGFRβ-Cre generated strong and relatively homogenous lacZ expression throughout adipose depots in adipocytes and mural cells (Fig. 4D). In contrast, SM22-Cre did not, although lacZ was expressed in a distinct subset of adipose depot vessels (Fig. 4D).

To assess the adipogenic potential of PDGFRβ-expressing mural cells, we isolated PDGFRβ-positive and -negative cells from white adipose tissues and other organs by FACS, cultured them in insulin, or transplanted them into nude mice (fig. S21). In both assays, the adipose depot $PDGFR\beta^+$ SV cells had higher (and substantially more) adipogenic potential than did $PDGFR\beta^-$ SV cells (Fig. 4E); this adipogenesis was stimulated by thiazolidinediones (TZDs), which are diabetes drugs that activate PPARγ (*23*) (Fig. 4F). In contrast, $PDGFR\beta^+$ cells isolated from other organs did not display such potential and were unresponsive to TZDs (Fig. 4F and fig. S22). Although we could identify sections that contained adipocytes in the non-adipose transplants, these adipocytes were GFP-negative (in contrast to adipocytes present in adipose depot SV $PDGFR\beta^+$ transplants) (fig. S22), apparently derived or recruited from host tissues. These data are consistent with the possibility that adipocyte progenitors reside as adipose depot mural cells with distinct properties such as adipogenic potential.

The intertwined epidemics of obesity and diabetes have led to a public health crisis that demands an improved understanding of adipocyte biology (*2*, *24*). Yet the identity of the adipocyte progenitors and their precise location has remained elusive. Exploiting genetic reporters, we show that the pool of murine white adipocyte precursors has largely been committed prenatally or just after birth. These precursors divide, maintain the progenitor pool, and produce adipocytes. Some of these progenitors appear to be mural cells that reside in the vasculature of adipose tissue; these results are supported by early electron micrographic studies (*25*, *26*). Thus, the adipose vasculature appears to function as a progenitor niche and may provide signals for adipocyte development.

Several earlier studies have documented an interplay between adipose tissue and the vasculature and shown that this interaction provides possible targets for obesity/diabetes therapies (*27*–*30*). The results described here add a fresh perspective to this interplay. In addition, they provide a foundation for further characterization of the adipose vascular niche and for prospective isolation of the adipocyte progenitors. Such experiments should help to establish whether intervention in adipose lineage formation can be an effective therapeutic approach for obesity and diabetes.

References and Notes

1. G. Ailhaud, P. Grimaldi, R. Negrel, *Annu. Rev. Nutr.* **12**, 207 (1992).
2. S. Gesta, Y. H. Tseng, C. R. Kahn, *Cell* **131**, 242 (2007).
3. S. Klaus, A. M. Cassard-Doulcier, D. Ricquier, *J. Cell Biol.* **115**, 1783 (1991).
4. M. A. Lazar, *Biochimie* **87**, 9 (2005).
5. S. R. Farmer, *Cell Metab.* **4**, 263 (2006).
6. A. Kistner *et al.*, *Proc. Natl. Acad. Sci. U.S.A.* **93**, 10933 (1996).
7. Materials and methods are available as supporting material on *Science* Online.
8. T. S. Yu, M. Dandekar, L. M. Monteggia, L. F. Parada, S. G. Kernie, *Genesis* **41**, 147 (2005).
9. P. Soriano, *Nat. Genet.* **21**, 70 (1999).
10. J. R. Cook, L. P. Kozak, *Dev. Biol.* **92**, 440 (1982).
11. S. Altiok, M. Xu, B. M. Spiegelman, *Genes Dev.* **11**, 1987 (1997).
12. E. D. Rosen, O. A. MacDougald, *Nat. Rev. Mol. Cell Biol.* **7**, 885 (2006).
13. T. Kanda, K. F. Sullivan, G. M. Wahl, *Curr. Biol.* **8**, 377 (1998).
14. T. Tumbar *et al.*, *Science* **303**, 359 (2004); published online 11 December 2003, 10.1126/science.1092436.
15. T. C. Otto, M. D. Lane, *Crit. Rev. Biochem. Mol. Biol.* **40**, 229 (2005).
16. J. M. Ntambi, K. Young-Cheul, *J. Nutr.* **130**, 3122S (2000).
17. R. A. Graves, P. Tontonoz, K. A. Platt, S. R. Ross, B. M. Spiegelman, *J. Cell. Biochem.* **49**, 219 (1992).
18. D. L. Jones, A. J. Wagers, *Nat. Rev. Mol. Cell Biol.* **9**, 11 (2008).
19. A. Armulik, A. Abramsson, C. Betsholtz, *Circ. Res.* **97**, 512 (2005).
20. A. Dellavalle *et al.*, *Nat. Cell Biol.* **9**, 255 (2007).
21. S. S. Foo *et al.*, *Cell* **124**, 161 (2006).
22. P. Boucher, M. Gotthardt, W.-P. Li, R. G. W. Anderson, J. Herz, *Science* **300**, 329 (2003).
23. J. M. Lehmann *et al.*, *J. Biol. Chem.* **270**, 12953 (1995).
24. P. G. Kopelman, *Nature* **404**, 635 (2000).
25. K. Iyama, K. Ohzono, G. Usuku, *Virchows Arch. B Cell Pathol.* **31**, 143 (1979).
26. S. Cinti, M. Cigolini, O. Bosello, P. Bjorntorp, *J. Submicrosc. Cytol.* **16**, 243 (1984).
27. M. A. Rupnick *et al.*, *Proc. Natl. Acad. Sci. U.S.A.* **99**, 10730 (2002).
28. M. G. Kolonin, P. K. Saha, L. Chan, R. Pasqualini, W. Arap, *Nat. Med.* **10**, 625 (2004).
29. L. E. Kuo *et al.*, *Nat. Med.* **13**, 803 (2007).
30. S. Nishimura *et al.*, *Diabetes* **56**, 1517 (2007).

31. We thank S. Kennedy, T. Wang, R. Adams, R. Evans, S. Kernie, L. Monteggia, M. Osawa, R. Perlingeiro, Q. LaPlant, and M. Iacovino, as well as members of the Graff lab. J.M.G. is a founder of Reata Pharmaceuticals, a privately held company designed to address unmet needs in cancer, neurodegenerative, and inflammatory conditions. This work was supported by NIH and the National Institute of Diabetes and Digestive and Kidney Diseases (grants 1R01DK064261 and 1R01DK066556) and the University of Texas Southwestern Medical Center Excellence in Education Fund. W.T., J.M.G., and the University of Texas Southwestern Medical Center may file a patent application related to the work reported here.

Supporting Online Material

www.sciencemag.org/cgi/content/full/1156232/DC1
Materials and Methods
Figs. S1 to S22
References

7 February 2008; accepted 4 September 2008
Published online 18 September 2008;
10.1126/science.1156232
Include this information when citing this paper.